

# Charge and Spin Dynamics of an Ordered Stripe Phase in $\text{La}_{1\frac{2}{3}}\text{Sr}_{\frac{1}{3}}\text{NiO}_4$ by Raman Spectroscopy

G. Blumberg,<sup>1,2,†</sup> M. V. Klein,<sup>1</sup> and S-W. Cheong<sup>3</sup>

<sup>1</sup>*NSF Science and Technology Center for Superconductivity and*

*Department of Physics, University of Illinois at Urbana-Champaign, Urbana, IL 61801-3080*

<sup>2</sup>*Institute of Chemical Physics and Biophysics, R vala 10, Tallinn EE0001, Estonia*

<sup>3</sup>*Bell Laboratories, Lucent Technologies, Murray Hill, NJ 07974 and*

*Department of Physics and Astronomy, Rutgers University, Piscataway, NJ 08855*

(July 7, 1997; to appear in Phys. Rev. Lett.)

For  $\text{La}_{1\frac{2}{3}}\text{Sr}_{\frac{1}{3}}\text{NiO}_4$  – a commensurately doped Mott-Hubbard system – charge- and spin-ordering in a stripe phase has been investigated by phononic and magnetic Raman scattering. Formation of a superlattice and an opening of a pseudo-gap in the electron-hole excitation spectra as well as two types of double-spin excitations – within the antiferromagnetic domain and across the domain wall – are observed below the charge-ordering transition. The temperature dependence suggests that the spin ordering is driven by charge ordering and that fluctuating stripes persist above the ordering transition.

PACS numbers: 71.45.Lr, 75.30.F, 74.70.Kb, 71.38.+i, 74.72.Dn, 78.30.Er, 74.25.Ha

The problem of doped Mott-Hubbard insulators has attracted much attention because of its relevance to the cuprate high temperature superconductors. Recent experiments on the doped lanthanum nickelate [1–3] and lanthanum cuprate [4–6] families of materials have established a new type of real space charge and spin ordering in topological phases. In the low-temperature stripe phase, the doped holes are concentrated in periodic antiphase domain walls for the intervening antiferromagnetic regions – see Fig. 1. These results appear to be consistent with the ideas of frustrated phase separations driven by the electron-electron interaction [7].

The stripe phase was first observed by electron diffraction [1] and by neutron scattering measurements [2] in the  $\text{La}_{2-x}\text{Sr}_x\text{NiO}_{4+\delta}$  system. Undoped  $\text{La}_2\text{NiO}_4$  is an antiferromagnetic charge-transfer insulator with a  $\text{O-}2p - \text{Ni-}3d$  gap of about 3.5 eV [8,9], twice as large as that in the isostructural  $\text{La}_2\text{CuO}_4$ . The ground state has spin  $\mathbf{S} = 1$  with holes localized on  $\text{Ni}^{2+}$  ( $x^2 - y^2, 3z^2 - 1$ ) sites. Introduction of holes into the  $\text{NiO}_2$  plane induces broad optical absorption in the infrared region below the charge-transfer gap, similar to the case of  $\text{La}_{2-x}\text{Sr}_x\text{CuO}_4$ , but unlike the cuprates the lanthanum nickelate remains insulating up to high doping levels and a Drude-type absorption band does not appear [8,10]. It has been suggested that the difference from the cuprates is the larger effect of the electron-phonon coupling [9,11] and stronger magnetic localization (less important spin fluctuations for spin-one system) [12]. The doped hole is nearly entirely localized on Ni and four nearest neighboring in-plane oxygen atoms. The high-frequency vibrations of the light oxygens participate in the electron-phonon interaction and form a small polaron. The spin of the additional hole is antiparallel to that of  $\text{Ni}^{2+}$  and leads to low spin on the doped nickel sites [9].

The neutron scattering measurement on  $\text{La}_{1\frac{2}{3}}\text{Sr}_{\frac{1}{3}}\text{NiO}_4$ ,

in which the number of doped holes per Ni site is  $1/3$ , has revealed that the system undergoes three successive transitions associated with quasi-two-dimensional commensurate charge and spin stripe ordering in the  $\text{NiO}_2$  planes [13]. The low-temperature phases are suggested to be static stripe lattice states with quasi-long-range in-plane charge correlation (See Fig. 1). Previously for the system with the same  $1/3$  doping anomalies associated with the charge ordering transition at  $T_{co} \approx 240$  K have been observed by electronic diffraction measurement [1] as well as in resistivity, magnetic susceptibility, sound velocity and specific heat [14,15]. In a recent optical study, Katsufuji *et al.* [16] observed that when temperature is decreased down to  $T_{co}$  the low-energy spectral weight below  $\sim 0.4$  eV becomes suppressed and is transferred to higher energy up to  $\sim 2$  eV. For  $T < T_{co}$  spectral weight below  $\sim 0.26$  eV becomes strongly reduced (A charge gap  $2\Delta(T)$  opens up.), and the missing spectral weight is also distributed over the higher energy region up to  $\sim 2$  eV. In this paper we study both charge and spin ordering by Raman spectroscopy. The data were taken on a  $\text{La}_{1\frac{2}{3}}\text{Sr}_{\frac{1}{3}}\text{NiO}_4$  single crystal grown as described in Ref. [13].

The Raman spectra were measured in the back-scattering geometry from the sample mounted in a continuous helium flow optical cryostat (Oxford Instruments). Throughout this study, we used linearly polarized 6471 Å excitation from a  $\text{Kr}^+$  laser. To reduce the heating by laser illumination we used about 5 mW of incident laser power focused onto a 50  $\mu\text{m}$  diameter spot on the *ab*-plane of the as grown mirror-like crystal surface. The incident photons were polarized along the direction  $45^\circ$  from the Ni-O bond. The crystallographic orientation was determined by X-ray Laue diffraction. The scattering photons were polarized either parallel ( $x'x'$  geometry) or perpendicular ( $x'y'$  geometry) to the incident photons

were collected and analyzed by a triple grating spectrometer with a liquid nitrogen cooled CCD detector. With assumed approximate  $D_{4h}$  symmetry, these two geometries correspond to spectra of  $A_{1g} + B_{2g}$  and  $B_{1g} + A_{2g}$  symmetry, respectively. The  $B_{2g}$  and  $A_{2g}$  components of the spectra ( $xy$  geometry) are found to be quite weak. Spectra were corrected for the spectral response of the spectrometer and the detector.

Figure 2 shows the Raman spectra for two polarizations as a function of temperature.

*Continuum.* At high temperatures spectra in both geometries show strong continuum intensity. In metals electronic Raman scattering by charge fluctuations arises from electron-hole excitations near the Fermi energy. For a normal metal within the Fermi liquid model the electronic Raman scattering has finite intensity only at very low frequencies. For strongly correlated systems, incoherent quasi-particle scattering leads to finite Raman intensity over a broad region of frequency [17,18], and the Raman intensity can be used as a measure of the incoherent quasi-particle scattering. At high temperatures the strong continuum scattering starts from very low frequencies, indicating gapless electron-hole excitations of the doped  $\text{La}_{1/3}\text{Sr}_{2/3}\text{NiO}_4$ . The low-frequency portion of the continuum intensity reduces with temperature reduction to 150 K indicating, in agreement with resistivity and optical conductivity studies [16], that a pseudo-gap opens up in the low-frequency electronic excitation spectra.

*Phonons.* Temperature dependence of optical-phonon structures provides evidence for the charge ordering transition at  $\sim 240$  K.

At room temperature  $\text{La}_{1/3}\text{Sr}_{2/3}\text{NiO}_4$  has the tetragonal  $\text{K}_2\text{NiF}_4$  structure with the space group  $I4/mmm$  [19], in which there should be four Raman-active phonon modes; Ni-O(2) and O(2)-La stretching along  $c$ -axis modes with the  $A_{1g}$  symmetry and the  $E_g$  symmetry O(2) and La vibrations along the  $a$ - or  $b$ -axis [20–23]. For the  $A_{1g}$  symmetry ( $x'x'$  geometry) the most intense peak at around  $500\text{ cm}^{-1}$  has been assigned to the oxygen stretching mode. This mode shows hardening with Sr doping [23]. We attribute the peaks around  $140\text{ cm}^{-1}$  to the La stretching mode. Above the charge ordering temperature all the observed modes are weak; the 140 and especially  $500\text{ cm}^{-1}$  modes are broad, indicating strong polaronic effects [9] and inhomogeneous charge distribution.

Conspicuous changes in phononic spectra are observed below  $T_{co}$ . The charge ordering gives rise to formation of a superlattice, triples the unit cell size and lowers the crystal symmetry (See Fig. 1). It leads to folding of phonon-dispersion branches and the appearance of new  $\Gamma$ -point Raman-active modes. In agreement with this picture, spectra exhibit a number of new sharp phononic modes at  $T < T_{co}$  [24]. The  $A_{1g}$  modes observed above  $T_{co}$  show significant sharpening and intensity en-

hancement at low temperatures. The Ni-O(2) stretching mode splits below  $T_{co}$  into two narrow peaks at 474 and  $515\text{ cm}^{-1}$  (Fig. 3) indicating that there are two nonequivalent Ni-O(2) bonds below the charge ordering temperature. The first might be assigned to the undoped Ni atoms between the domain walls, and the second to the Ni atoms on the walls where doped holes are tightly localized (See Fig. 1). Katsufuji *et al.* observed splitting below  $T_{co}$  of the IR-active  $E_u$  symmetry  $355\text{ cm}^{-1}$  in-plane Ni-O(1) bending mode [16] that also can be understood in terms of two types of Ni-O(1) bonds in the charge-ordered phase.

In the Fig. 4 we show the temperature dependence of the Ni-O(2) stretching mode Raman intensity integrated between 400 and  $640\text{ cm}^{-1}$  above the continuum. Analogous temperature dependence has been observed for other phononic modes. The intensity shows strong enhancement below  $T_{co}$ , and its temperature dependence is similar to the temperature dependence of the gap magnitude  $2\Delta(T)$  from optical measurements [16] that has been suggested to be a relevant order parameter for the charge-ordered phase. The presented Raman spectra are excited with 1.9 eV photons, energy in the region where the spectral weight is transferred when the charge gap opens up below  $T_{co}$  [16]. Hence, the intermediate state of the scattering process is in resonance with states that are sensitive to the charge ordering transition. The oxygen and La phonon modes, on the other hand, modulate the atomic displacement to produce the commensurate charge-ordered state. Therefore, the resonant Raman intensity of the phononic modes that participate in the charge ordering transition is coupled *via* the intermediate state to the order parameter  $2\Delta$ .

*Spin excitations.* Short wavelength antiferromagnetic fluctuations, which may exist without long-range antiferromagnetic order, can be probed by Raman scattering. The Raman process takes place from antiferromagnetic ( $\mathbf{S} = 1, S_z = \pm 1$ ) ground state *via* a photon-stimulated virtual charge-transfer excitation that exchanges two spins on nearest neighbor Ni sites in an intermediate two singlets ( $\mathbf{S} = 0, S_z = 0$ ) state (each of two exchanged spins compensates with the remaining spins on the same sites) [18], and then to a final triplet ( $\mathbf{S} = 1, S_z = 0$ ) state. This process may also be described as creation of two interacting magnons.

The undoped  $\text{La}_2\text{NiO}_4$  antiferromagnetic insulator has been studied by Sugai *et al.* [25]. The  $B_{1g}$  spectra exhibits a band peaked at about  $1640\text{ cm}^{-1}$ . This band has been assigned to scattering by two-magnons. For  $\mathbf{S} = 1$  system two-magnon excitation requires about  $\sim 7J$  energy due to increase of the Heisenberg interaction  $J \sum_{\langle i,j \rangle} (\mathbf{S}_i \cdot \mathbf{S}_j - \frac{1}{4})$  [ $J$  is spin superexchange constant,  $\mathbf{S}_i$  is the spin on site  $i$  and the summation is over near-neighbor Ni pairs.]. Thus for the antiferromagnetic insulators the two-magnon peak position yields an estimate of  $J \approx 240\text{ cm}^{-1}$ .

For doped  $\text{La}_{1-\frac{2}{3}}\text{Sr}_{\frac{1}{3}}\text{NiO}_4$  we have not observed a band near  $1640\text{ cm}^{-1}$  at any temperature. Instead, at low temperature the spectra in  $x'y'$  polarization exhibit two bands peaked at  $\sim 720$  and  $\sim 1110\text{ cm}^{-1}$ . We interpret these two bands as double-spin excitations with reduced energy due to reduction in the number of magnetic nearest neighbors (broken magnetic bonds) in the vicinity of charge domain walls [26]. The first band is double-spin excitation within the antiferromagnetic domain with Heisenberg magnetic energy price of  $\sim 3J$ , and the second one across the domain wall with  $\sim 4J$  energy, respectively (See Fig. 1). The observed reduction of the two-magnon energy relative to the energy in the undoped antiferromagnetic insulators is consistent with the neutron scattering study of  $\text{La}_2\text{NiO}_{4+\delta}$  by Tranquada *et al.* [27] where it was found that the spin-wave velocity for excitations propagating parallel to the stripes in  $\delta = 0.133$  sample is  $\approx 60\%$  of that in undoped  $\text{La}_2\text{NiO}_4$ .

The temperature dependence of the magnetic scattering intensity integrated above the continuum up to  $1400\text{ cm}^{-1}$  and the intensity portion under the second peak (integrated between  $875$  and  $1400\text{ cm}^{-1}$ ) are shown in the Fig. 4. Above  $T_{co}$  the magnetic excitations are overdamped; however, a weak peak about  $600\text{ cm}^{-1}$  is seen on the strong continuum background suggesting that the fluctuating stripes exist above the charge-order transition. When the charge gap  $2\Delta$  opens up below  $T_{co}$ , the  $720\text{ cm}^{-1}$  two-magnon band, freed from the damping, emerges from the overdamped excitation. The temperature dependence of the magnetic scattering intensity and shape indicates that the antiferromagnetic ordering within the undoped region is retarded relative to the charge ordering transition. The short range antiferromagnetic order begins to be established at perhaps about  $200\text{ K}$ , a temperature where the long range static charge correlations have been observed by elastic neutron scattering [13], and the quasi-one-dimensional antiferromagnetic ordering continues down to the lowest temperature. The  $1110\text{ cm}^{-1}$  band intensity indicates that the relative  $\pi$ -phase shift between the antiferromagnetic regions becomes established at lower temperatures.

In summary, lattice and spin dynamics of  $\text{La}_{1-\frac{2}{3}}\text{Sr}_{\frac{1}{3}}\text{NiO}_4$ , which undergoes charge and spin ordering transitions starting from  $240\text{ K}$ , are investigated by Raman spectroscopy. In the high-temperature phase the Raman continuum demonstrates strong incoherent quasi-particle scattering and gapless electron-hole excitation. Below  $240\text{ K}$  a pseudo-gap opens up in the low-frequency electronic excitations. The charge ordering gives rise to formation of a superlattice that is observed in splitting of optical phonon and appearance of new Raman-active modes. The resonance Raman scattering intensity of these phononic modes reflects redistribution of the electronic spectra caused by charge ordering. The magnetic Raman scattering shows two bands

corresponding to photon induced double spin excitation within the antiferromagnetic domain and across the domain wall. Their temperature dependence suggests that the magnetic order is driven by charge order and reflects the temperature dependence of the short range magnetic correlations within antiferromagnetic domain as well as across the domain wall in the stripe phase. Overdamped short-range antiferromagnetic correlations are observed above  $T_{co}$ , suggesting fluctuating stripes in the high temperature phase.

We acknowledge discussions with V.J. Emery, S.A. Kivelson, M. Salamon and J. Tranquada. This work was supported by NSF grant DMR 93-20892 and cooperative agreement DMR 91-20000 through the STCS.

---

<sup>†</sup> Electronic address: blumberg@uiuc.edu

- [1] C. H. Chen, S.-W. Cheong, and A. S. Cooper, Phys. Rev. Lett. **71**, 2461 (1993).
- [2] J. M. Tranquada, D. J. Buttrey, V. Sachan, and J. E. Lorenzo, Phys. Rev. Lett. **73**, 1003 (1994).
- [3] V. Sachan *et al.*, Phys. Rev. B **51**, 12742 (1995); J. M. Tranquada, J. E. Lorenzo, D. J. Buttrey, and V. Sachan, Phys. Rev. B **52**, 3581 (1995).
- [4] J. Tranquada *et al.*, Nature **375**, 561 (1995).
- [5] J. Tranquada *et al.*, Phys. Rev. B **54**, 7489 (1996); Phys. Rev. Lett. **78**, 338 (1997).
- [6] S.-W. Cheong *et al.*, Phys. Rev. Lett. **67**, 1791 (1991); T.E. Mason *et al.*, *ibid.* **68**, 1414 (1992); T. R. Thurston *et al.*, Phys. Rev. B **46**, 9128 (1992).
- [7] V.J. Emery and S.A. Kivelson, Physica C **209**, 597 (1993); *ibid.* **235-240**, 189 (1994); U. Löw *et al.*, Phys. Rev. Lett. **72**, 1918 (1994); J. Zaanen, M.L. Horbach, and W. van Saarloos, Phys. Rev. B **53**, 8671 (1996); V.J. Emery, S.A. Kivelson, O. and Zachar, *ibid.*, 6120 (1997) and references therein.
- [8] T. Ido *et al.*, Phys. Rev. B **44**, 12094 (1991).
- [9] V.I. Anisimov *et al.*, Phys. Rev. Lett. **68**, 345 (1992).
- [10] X.-X. Bi, P.C. Eklund, and J.M. Honig, Phys. Rev. B **48**, 3470 (1993).
- [11] J. Zaanen and P.B. Littlewood, Phys. Rev. B **50**, 7222 (1994).
- [12] S.A. Kivelson and V.J. Emery in Strongly correlated Electronic Materials: The Los Alamos Symposium 1993 (eds. K.S. Bedell *et al.*) 619-656 (Addison-Wesley, Reading, MA, 1994).
- [13] S.-H. Lee and S.-W. Cheong, Phys. Rev. Lett. **79**, 2514 (1997).
- [14] S.-W. Cheong *et al.*, Phys. Rev. B **49**, 7088 (1994).
- [15] A.P. Ramirez *et al.*, Phys. Rev. Lett. **76**, 447 (1996).
- [16] T. Katsufuji *et al.*, Phys. Rev. B **54**, R14 230 (1996).
- [17] C. M. Varma *et al.* Phys. Rev. Lett. **63**, 1996 (1989).
- [18] B.S. Shastry & B.I. Shraiman Phys. Rev. Lett. **65**, 1068 (1990); Intern. J. Mod. Phys. B **5**, 365 (1991).

- [19] S.H. Han *et al.*, Phys. Rev. B **52**, 1347 (1995).
- [20] F.E. Bates and J.E. Eldridge, Solid State Comm. **72**, 187 (1989).
- [21] G. Burns *et al.*, Phys. Rev. B **42**, 10 777 (1990).
- [22] A. de Anders *et al.*, J. Phys.: Condens. Matter **3**, 3813 (1991).
- [23] M. Udagawa *et al.*, Phys. Rev. B **47**, 11 391 (1993).
- [24] The detailed assignment of these new modes is yet to be made.
- [25] S. Sugai *et al.*, Phys. Rev. B **42**, 1045 (1990); Physica C **185-189**, 895 (1991).
- [26] The spin superexchange across the domain wall is expected to be small.
- [27] J.M. Tranquada, P. Wochner, and D.J. Buttrey, Phys. Rev. Lett. **79**, 2133 (1997).

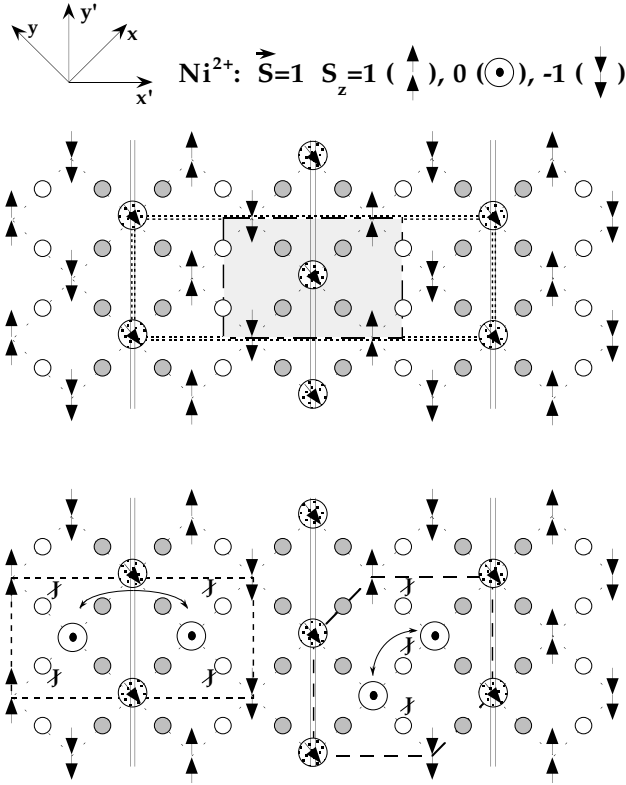


FIG. 1. The low-temperature stripe phase for 1/3 doping. Arrows indicate uncompensated spins on Ni sites; circles indicate oxygen sites; shaded circles indicate locations of doped holes on oxygen and Ni sites (the orientation of remaining spin on the Ni site is frustrated). Dashed lines trace the bonding paths of the square lattice (the unit cell of the tetragonal high-temperature phase). Double lines indicate position of the domain walls. The low-temperature charge unit cell is shown by shaded area while double broken lines outline a magnetic unit cell. The lower panel illustrates two types of double-spin excitations: the double-spin excitation within an antiferromagnetic domain breaks three magnetic bonds (broken bonds are shown as //), while the excitation across the domain wall breaks four bonds [26].

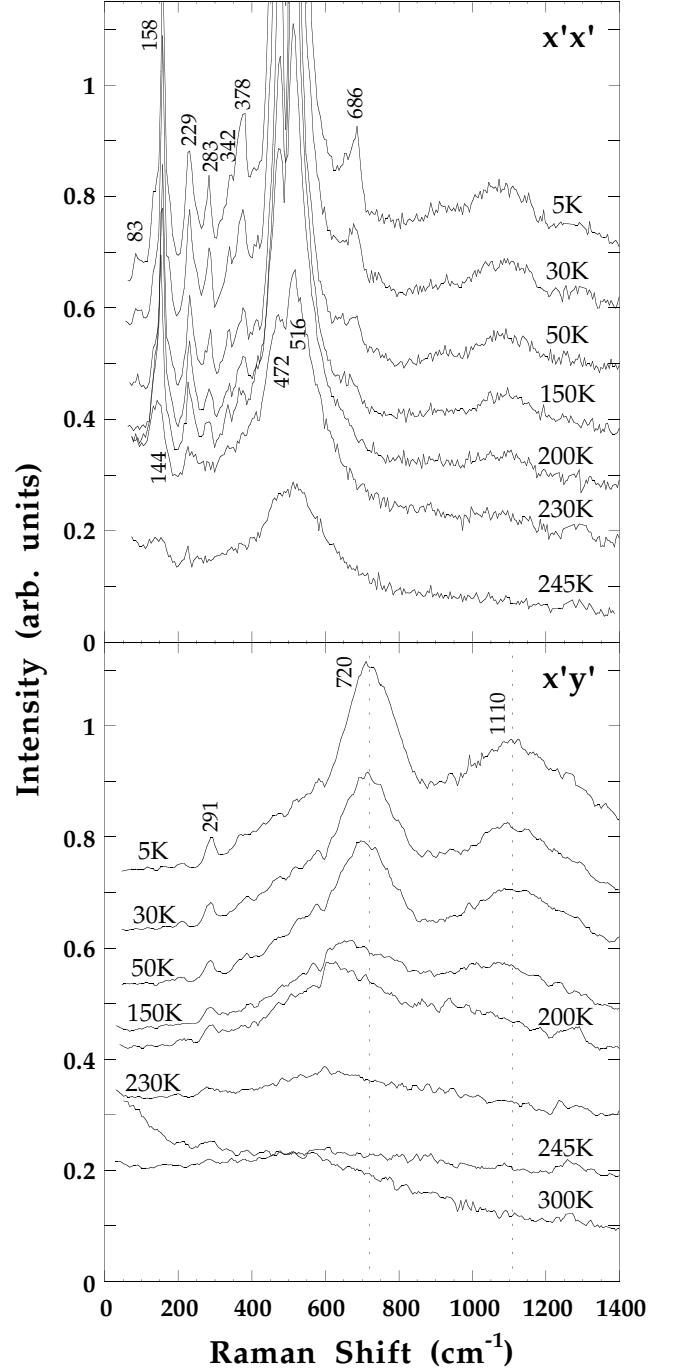


FIG. 2. Temperature dependent Raman scattering spectra for  $x'x'$  and  $x'y'$  polarization. Baselines are shifted by one tick.

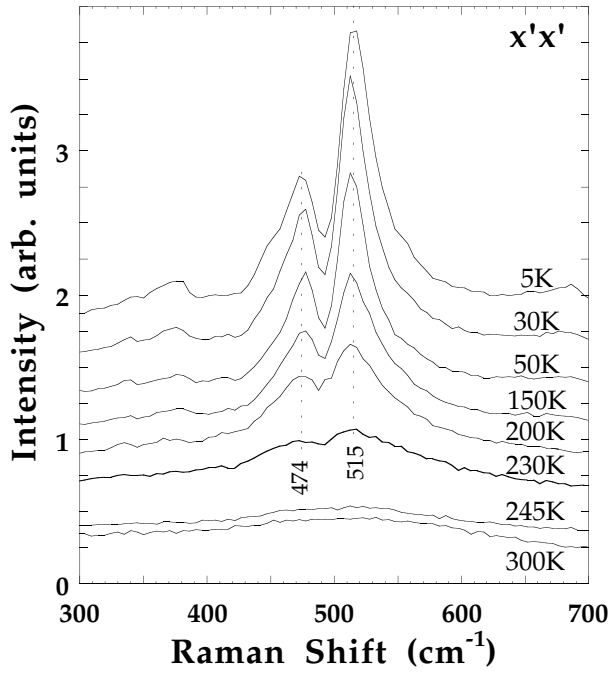


FIG. 3. Temperature dependent Raman scattering spectra for  $x'x'$  polarization. Baselines are shifted by one tick. The 474 and 515  $\text{cm}^{-1}$  phonons are assigned to Ni-O(2) stretching modes on undoped and doped sites.

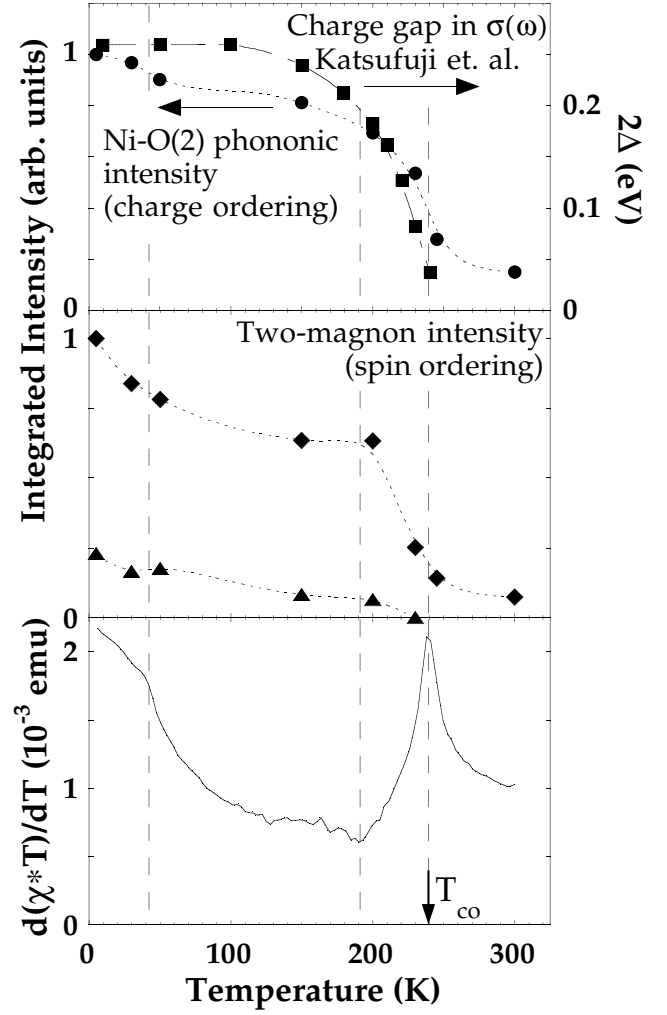


FIG. 4. Temperature dependence of the Ni-O(2) stretching modes intensity (See Fig. 3) integrated between 400 and 640  $\text{cm}^{-1}$  above the continuum (circles) shown together with the charge gap in optical conductivity from Ref. [16] (squares); the magnetic scattering intensity in both 720 and 1110  $\text{cm}^{-1}$  bands (See Fig. 2) integrated above the continuum up to 1400  $\text{cm}^{-1}$  (diamonds) and the intensity portion under the 1110  $\text{cm}^{-1}$  peak integrated between 875 and 1400  $\text{cm}^{-1}$  (triangles); also anomalies in  $d(\chi T)/dT$  [13] are shown for comparison.